CMS Physics Analysis Summary

Contact: cms-pag-conveners-exotica@cern.ch 2009/07/03

Searching for Stopped Gluinos during Beam-off Periods at CMS

The CMS Collaboration

Abstract

In this note we describe plans for a search for long-lived particles which have become stopped by the CMS detector. We will look for the subsequent decay of these particles during time intervals where there are no pp collisions in CMS. In particular, we will search for decays during gaps between crossings in the LHC beam structure as well as the inter-fill period between the beam being dumped and re-injection. We record such decays with dedicated calorimeter triggers. For models, such as split-susy gluinos, the relatively large cross-section combined with the relatively good stopping power of CMS, yields a significant number of triggerable decays. If LHC instantaneous luminosity approaches $10^{32} cm^{-2} s^{-1}$ in 2009-10, 5 sigma significance can be established in a matter of days since these decays occur on top of a negligible background.

1 Introduction

There are a number of new physics scenarios which predict the existence of new heavy quasi-stable charged particles. One such theoretical scenario is "split supersymmetry" [1]. Just like in many more traditional supersymmetric models, in split SUSY, copious gluino production is expected at the LHC via $gg \to \tilde{g}\tilde{g}$ with rates approaching 1 Hz (at design luminosity) for the lightest gluino masses. Unlike traditional SUSY, however, there is a very large mass splitting between the new scalars and new fermions from which the theory gets its name. Gluinos can thus only decay[1] through a highly virtual squark. The lifetime of the gluino can thus be quite long; the gluino may well be stable on typical CMS [2] experimental timescales. Existing experimental constraints on the value of this lifetime are weak [3].

If long-lived gluinos are produced at CMS, they will hadronize into $\tilde{g}g, \tilde{g}q\bar{q}, \tilde{g}qqq$ states which are collectively known as "R-hadrons". Some of these gluino bound states will be charged whilst others will be neutral. Those which are charged will lose energy via ionization as they traverse the CMS detector. For low-β R-hadrons, this energy loss is sufficient to bring a significant fraction of the produced particles to rest inside the CMS detector volume [4]. These "stopped" R-hadrons will decay seconds, day, or weeks later. These decays will be out-of-time with respect to LHC collisions and may well occur at times when there are no collisions (e.g. beam gaps) or when there is no beam in the LHC machine (e.g. interfill period). The observation of such decays, in what should be a quiet detector save for the occasional cosmic ray, would be an unambiguous discovery of new physics.

We have devised and implemented a search strategy that enables us to use CMS to detect such decays.

2 Signal Simulation

Stopped particles will decay spherically (since they are at rest) from a location displaced by meters from the nominal origin of CMS. The geometry of such events is thus very different to the typical pp collision for which the CMS detector was designed. In order to study the properties of these unusual events (and in particular to learn how to trigger on and reconstruct them) we used a custom simulation. The simulation of a particle which may decay seconds, hours, or days after its production involves timescales which are significantly beyond those which occur in "normal" simulations. We solved this problem by factorising the simulation into three phases. In Phase 1, we simulate the passage of stable particles through the CMS detector, keeping track of the energy loss of these particles at each space-time point, and noting if (and when) the kinetic energy has fallen to zero, i.e. the particle has come to rest. We repeat this process many times and in this manner obtain a 3D probability density function for the stopping of such a particle at an arbitrary location within the CMS detector. In Phase 2, we sample this "stopping map" to obtain a probable stopping location. We then use a particle gun to generate a particle at rest, translate it's production vertex to the stopping location, and allow it to decay instantaneously. Phase 3 simulates the timing of this decay relative to the LHC beam clock.

For Phase 1, we generate gluino events at $\sqrt{s} = 10$ TeV using PYTHIA to simulate the dominant leading order production processes, $q\bar{q} \to \tilde{g}\tilde{g}$ and $gg \to \tilde{g}\tilde{g}$. The lifetime of the gluino is set such that it is stable and we scan gluinos masses from $m_{\tilde{g}} = 200 - 1200$ GeV. PYTHIA also hadronizes the produced gluino into R-hadrons.

[1] This statement assumes R-parity is conserved.

These R-hadrons are passed to the CMS simulation where GEANT4 simulates the interaction of the generated R-hadrons with the CMS detector. To accomplish this, GEANT4 employs the so-called "cloud model" for the interaction of stable heavy hadrons with matter [5].

Eventually, the R-hadron either stops in the material of the detector, or exits it. In former case the coordinates of the stopping point, (x, y, z), are recorded. The process is repeated until a sufficient number of stopping points are recorded to adequately populate a 3D stopping map. The total stopping efficiency for a given mass is also computed for use in Phase 3.

Figure 1 shows distributions of stopping points[2] for $m_{\tilde{g}} = 300$ GeV. The material structure of the CMS detector is clearly seen in these distributions. Figure 2 presents the stopping probability as a function of gluino mass. Nuclear interactions (NI) which depend on the cloud model introduce an uncertainty in the stopping efficiency. We therefore show the stopping probability do to much more certain electromagnetic interactions (EM) alone in addition to the stopping efficiency due to the combined effects of EM+NI.

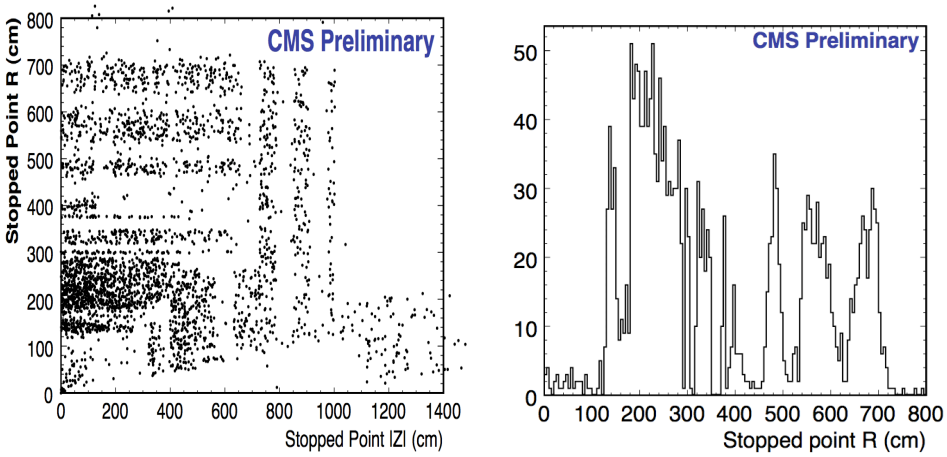

Figure 1: R-hadron stopping points for $m_{\tilde{g}} = 300$ GeV, and $\sqrt{s} = 10$ TeV. In the $R - |z|$ plane (left) and for the barrel only in $|z|$ (right).

Having obtained the stopping map in Phase 1, we proceed to simulate the decay of the stopped R-hadron in Phase 2. We run PYTHIA as a particle gun which produces R-hadrons at $(0, 0, 0)$ as normal. However, we randomly sample the stopping map obtained in Phase 1 to obtain a probability weighted stopping location $(x_{stop}, y_{stop}, z_{stop})$, and subsequently translate the R-hadron from its nominal vertex position to the selected stopped location.

The lifetime of the gluino is set such that it will decay instantaneously. The kinematics of a R-hadron decay is dominated by the properties of the gluino and neutralino - the spectator quarks do not play a significant role. These spectator quarks can not be ignored, however, as they participate in hadronization of produced gluon or quarks. We developed and implemented customized decays table to correctly describe these decays where a white R-hadron decays into a colored gluino, quark, and diquark with appropriate color structure. For example:

$$\Delta_{\tilde{g}}^{++} \rightarrow \tilde{g}\, u(uu) \rightarrow g\, \tilde{\chi}_1^0\, u(uu)$$

Finally, PYTHIA hadronizes the decay products, and parton-showering proceeds as usual. These

[2] For a higher statistics version of the Rz plot as well as the xy view, see Appendix A.

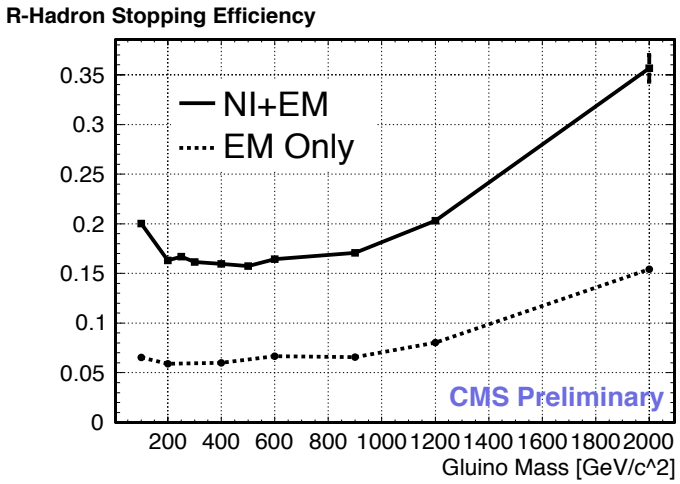

Figure 2: Probability for the produced R-hadron to stop anywhere inside the CMS detector for different gluino masses, and $\sqrt{s} = 10$ TeV. The solid line show stopping probability for both electromagnetic and nuclear interactions, while the dashed line shows that for electromagnetic interactions only.

fully simulated stopped gluino events are passed on to the full trigger emulation, and default reconstruction, and are analysed as normal Monte Carlo data. With Phase 2 of the simulation we are thus able to estimate the trigger and reconstruction efficiencies of our online and offline cuts.

For Phase 3, we wrote a toy Monte Carlo simulation in order to determine how often a stopped-gluino decay will occur during our trigger window. We define our trigger window to be one that occurs during a beam gap or during an interfill period. The interplay between collision time, stopped particle lifetime and our trigger window is illustrated by the cartoon in Figure 3 which shows the number of stopped undecayed particles in CMS at a given time. Particles are produced when there are collisions increasing the number of stopped undecayed particles, but this is counterbalanced by the decay of those particles. For running periods long relative to the lifetime of the gluino, the number of particles approaches saturation at $\mathcal{L}\sigma\tau$. When the beam is off, particle production obviously stops and all the number of stopped particles falls off exponentially in accordance with its lifetime[3].

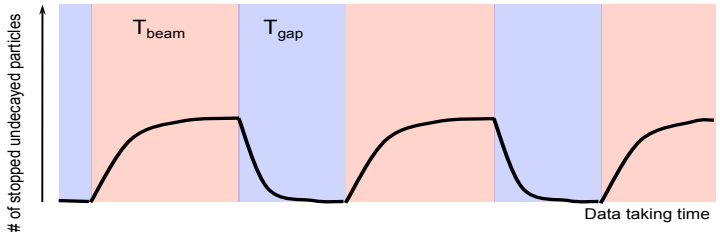

Figure 3: Cartoon illustrating number of stopped undecayed particles as a function of time.

Phase 3 of our simulation takes as input the stopping efficiency determined in Phase 1 and the combined trigger times reconstruction efficiency obtained in Phase 2. These efficiencies are

[3]The stopped particle lifetime can itself be measured by fitting this exponential decay, provided a period with no collisions of suitable duration is available.

multiplied together and then multiplied by the production cross-section, instantaneous luminosity, and a running time to determine the total number of detectable decays. Next, the simulation determines when these decays take place. The simulation does the same for background events for which we use the rate of instrumental noise and cosmics measured with pre-collision data recorded by CMS in Autumn 2008 (during CRAFT, the"Cosmic Run at Four Tesla"). Finally, the simulation determines whether each event takes place at a sensitive time (during the trigger window) and is thus "observable" or not. The number of observable events is recorded and a counting experiment is performed, the results of which are presented in Section 7.

3 Stopped Particle Experimental Signature

We use the simulation described in the previous sections to investigate the way in which our atypical signal develops in the CMS detector in order to devise how to trigger on these events. As show in Figure 2, a significant fraction of R-hadrons will stop in the calorimeters. We thus start our investigation with the energy deposited in the ECAL and HCAL during the subsequent decay of these R-hadrons. The plots and numbers given in this section are presented for $m_{\tilde{g}} = 300$ GeV and $M_{\chi^0} = 50$ GeV. Results for a range of these parameters will be presented later. Event displays for a typical signal event are shown in Figure 4. Most events show a clear, high energy jet centered around the decay vertex.

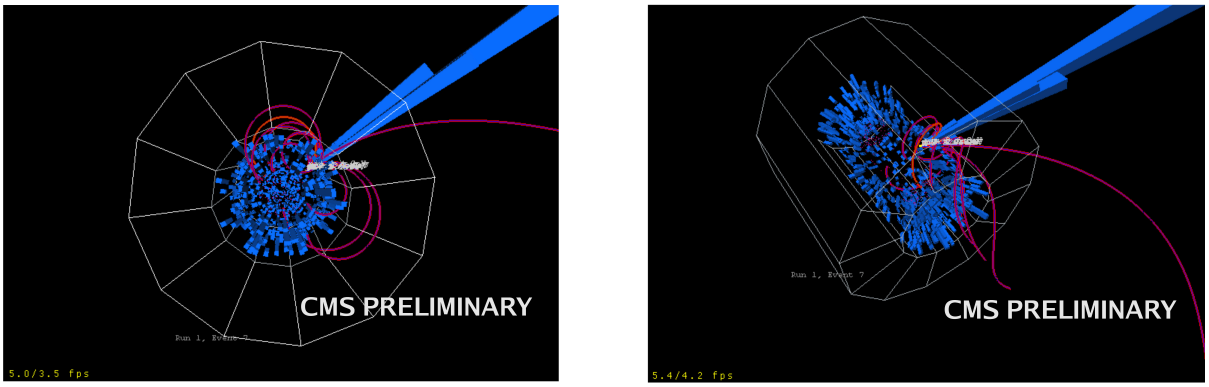

Figure 4: Event display for a particle decaying from within the HCAL, giving a sharp, high energy jet. The tracks shown are the paths simulated particles rather than reconstructed quantities.

4 Triggering Strategy

We will trigger on the energy our signal deposits in the calorimeter. For this a normal jet trigger will suffice. What is novel, however, is that we only want to fire this jet trigger during time buckets in which a pp collision did not occur in CMS. In addition to providing a collision background free environment, this allows us to have a low threshold (without a prescale).

We plan to run this trigger *any time* there is no beam in the LHC, i.e. between fills and during shut-downs. A search conducted during these time periods will be sensitive to lifetimes ranging from hours to weeks. In order to gain sensitivity to much shorter lifetimes (μs to minutes), we will also run this trigger *during* an LHC fill.

There are numerous periods during the LHC orbit in which no pp collisions occur in CMS. These gaps have lengths of 0.2 μs, 1 μs and 3 μs, and in total account for around 20% of the LHC orbit. We utilise information from the beam position and timing monitors, to trigger on

decays during these gaps. These monitors are positioned 175 m around the LHC ring either side of the CMS interaction region, and produce a signal when an LHC bunch passes the monitor. The coincidence of signals from both BPTX indicates bunches passing in both directions, and hence the possibility for a pp collision. For the stopped gluino search, we require a jet trigger together with the condition that neither monitor indicate a passing bunch. This ensures that the trigger will not fire on jets produced from pp collisions or any other beam related particle activity.

Our L1 trigger is the logical AND of the lowest threshold (10 GeV) normal jet trigger with the no beam condition. We have measured the rate of this trigger in CRAFT data to be $\sim$ 200 Hz. When the LHC is operating, the rate of this trigger will be reduced depending on the number of filled LHC bunches (which will vary over the commissioning period of the LHC).

Although the L1 trigger rate is relatively low, further rejection is required to reduce the rate to an acceptable level, of order 1 Hz. The main contribution to the L1 rate is HCAL electronics noise. The HLT path first applies filters designed to reject such noise, while maintaining good efficiency for signal. Next, jets are reconstructed, and a 20 GeV threshold is applied to the leading jet energy; this is the main control of HLT output rate. The L1+HLT trigger rate is shown as a function of the final jet energy threshold, in Figure 5a. The efficiency for signal ($m_{\tilde{g}} = 300$ GeV, $M_{\tilde{\chi}^0} = 50$ GeV) is shown as a function of jet energy threshold in Figure 5b.

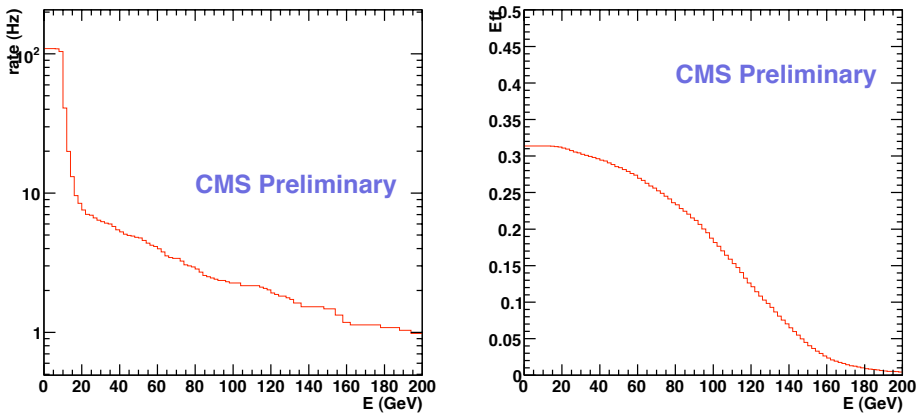

Figure 5: a) L1+HLT trigger rate from CRAFT data and b) simulated signal efficiency (with respect to all stopped particles), as functions of jet energy threshold, after emulation of L1 and upstream HLT cuts.

5 Backgrounds

As discussed above, the stopped particle search data will be recorded in periods where there are no collisions in CMS. Consequently, the only significant physics background source will be cosmic rays. In addition to physics sources of background we will also have instrumental backgrounds. We have used CRAFT data to measure both these backgrounds. The CRAFT data provides an ideal control sample since it was recorded under very similar conditions to those we will encounter when we search for stopped gluinos, yet there can be no signal contamination since no pp collisions have occurred (and hence no gluinos have been produced). Although the detector operating conditions used to take the CRAFT background sample are not expected to differ from those that will be used with LHC beam, various modifications and

improvements have been made to the detector since CRAFT. The background measurement will therefore be re-established during further data taking planned by CMS before the first LHC collisions.

When running the trigger during a fill, we expect some beam related backgrounds, due to beam halo, or particles in unfilled "buckets". Beam halo particles may cause a trigger if they deposit energy in HCAL that is identified by the readout as coming from an unfilled RF bucket 25ns before a real bunch-crossing. Particles in unfilled bunches may be present at levels below the BPTX threshold, and thus may cause a trigger if they interact with the beampipe, or gas, in the CMS interaction region. pp collisions between such particles are extremely unlikely since they are off beam momentum and diffusely distributed. These beam backgrounds cannot be measured without circulating beam, but we have several means of removing them, should they become of concern. Both types of event have features very different from a stopped particle decay; beam halo events will be associated with a track in one or other muon endcap, beampipe or beamgas events will be associated with tracks in the tracker pointing to a vertex inside, or on, the beampipe. In addition, beam halo may be removed by masking time buckets adjacent to filled bunches, either offline or in the trigger. We assume for the purposes of this study, that beam backgrounds can be ignored.

6 Offline Analysis

In order to reduce the instrumental background to acceptable levels we employ both topological and timing based cuts. Firstly, we restrict our search to jets in the HCAL barrel only, i.e. we require $|\eta| < 1.3$. Since most gluino bound states are produced centrally due to their high mass, the endcaps and forward calorimeters do not contribute much to the signal rate.

We also make several cuts on the shape and magnitude of HCAL energy deposits in order to discriminate against HCAL instrumental noise which gives rise to jets with unusual shapes. To remove events where a single HCAL channel has fired due to data corruption or single channel noise we veto events with 90% of the energy deposit in three or less towers. We also veto events where the leading jet does not have 60% of its energy in the leading 6 or less calorimeter towers. To reject fluctuations over the jet threshold and energy deposits from MIP's we make a hard cut on the reconstructed jet energy at 50 GeV. In order to further reject cosmic ray events we run the cosmic muon reconstruction algorithms (rather than the default muon reconstruction for pp collisions) and veto events containing a muon. The background rate after applying this combination of cuts is 0.0049 Hz (0.09% of events passing the HLT), and 61% of signal events passing the HLT are preserved.

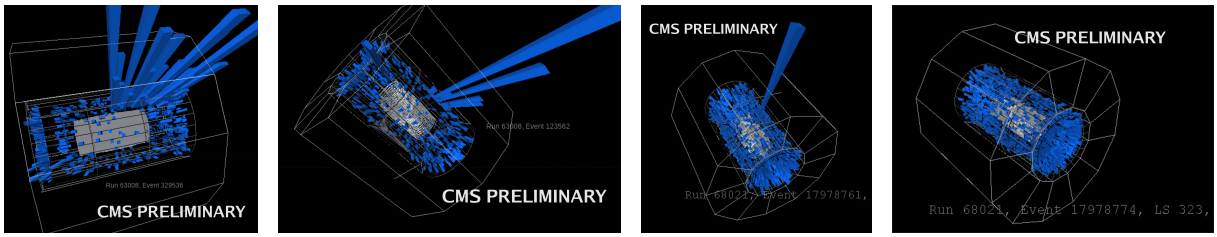

Figure 6: Examples of noise events removed by cuts.

The HCAL electronics have a well defined time response to charge deposits generated by showering particles. This pulse shape is used to distinguish deposits from real physics processes from pulses generated by electronics noise, which may not have a physics-like time profile.

The physical pulse has some notable properties which can be used to distinguish it from the

noise pulses. There is a clear peak bunch crossing, (BX_{Peak}), significant energy in one bunch crossing before the peak (BX_{Peak-1}) and an exponential decay for several BX's following the peak. We use the ratios $R_1 = BX_{peak+1}/BX_{peak}$ and $R_2 = BX_{peak+2}/BX_{peak+1}$ to characterize the exponential decay. We also reject noise events based on the presence of energy in the earliest or latest BX's, which we denote $BX_{1+2+9+10}$, since a physical pulse only populates BX_{peak-1},BX_{peak},BX_{peak+1},BX_{peak+2}.

We have tuned our selection based on both the pulse shape predicted by our Monte Carlo simulation. To cross-check these cuts against a real physical pulse shape, we calculate the efficiency against a sample of events from CRAFT taken with a muon trigger, that also contain a reconstructed cosmic muon and a significant energy deposit in HCAL.

Applying these timing cuts preserves 84% of Monte Carlo stopped gluino events which survive the topological cuts described previously. 91% of the remaining background events are rejected and 50% of the CRAFT events where a cosmic muon deposits high energy in HCAL remain.

6.1 Final Background Rate and Signal Efficiency

The final background rate after all cuts is 0.00039 Hz. The final signal efficiency (for $m_{\tilde{g}}$ = 300 GeV, $M_{\tilde{\chi}}$ = 50 GeV) is 16.4% of all stopped particles, or 52% of all triggered events. The efficiencies of all online and offline cuts are summarized in Table 1

Table 1: Noise rates and signal efficiencies after each online and offline cut. Efficiencies are given as a percentage of all stopped particles. Errors on the trigger rates are statistical uncertainties.

Cut	Background Rate	Signal Efficiency (% of Stopped)
L1 Rate (online)	200 ± 2.9 Hz	35.6 %
HLT Rate (online)	5.2 ± 0.25 Hz	31.8 %
$\lvert\eta_{jet}\rvert < 1.3$	1.39 Hz	26.1 %
Jet $n90 > 3$	0.218 Hz	24.8 %
Jet $n60 < 6$	0.076 Hz	21.7 %
$E_{jet} > 50$ GeV	0.024 Hz	20.3 %
Muon Veto	0.0049 Hz	19.4%
$0.15 < R_1$ and $0.10 < R_2 < 0.50$	0.00063 Hz	16.5%
$0.4 < BX_{Peak}$ / Total Energy < 0.7	0.00050 Hz	16.5%
$BX_{1+2+9+10}$ / Total Energy < 0.1	0.00039 Hz	16.4%

7 Split Supersymmetry Discovery Potential

In this section, we use the measured background rate from CRAFT and the estimated signal rate from Phase 1 + Phase 2 of our simulation, (after all cuts as described in Section 6) as input to Phase 3 of our simulation which we use to quantify our signal significance over background by performing a large number of pseudo-experiments.

The production cross-section for 300 GeV gluinos ($q\bar{q} \rightarrow \tilde{g}\tilde{g}$ and $gg \rightarrow \tilde{g}\tilde{g}$) at $\sqrt{s} = 10$ TeV is 0.5 nb. We consider an instantaneous luminosity scenario of 10^{32} cm^{-2} s^{-1}, and scan gluino lifetimes from 1 μs to 1 week. We assume the LHC is filled with 2808 bunches per beam, and that the operating cycle consists of a 12 hour fill followed by a 12 hour interfill period. We also assume that the trigger is allowed to run for the entire interfill period.

At the present time, we only present the results of a simple counting experiment. Nevertheless, even with only a counting experiment, there is the potential to make a 5 sigma discovery over 12 orders of magnitude in lifetime in a matter of days with an instantaneous luminosity of 10^{32} cm^{-2}. To avoid integrating excess background in the interfill experiment, we count within a time-window optimised for sensitivity to a particular gluino lifetime hypothesis. We find this time-window to be $1.256 \times \tau_{\tilde{g}}$. Figure 7 shows the discovery reach during both beam gaps and interfill periods in a combined counting experiment. The beamgap experiment is sensitive to lifetimes in the range 1 μs to hours, and the interfill experiment is sensitive to lifetimes ranging from hours to weeks. It should be noted that the 1 ms curve is representative of a very large range of lifetimes, from 10 μs to 100 s (which are not shown, for clarity). In this range, the lifetime is longer than the longest gap in the LHC beam structure, yet short enough that the interfill experiment provides little live time due to the time-window. This regime is optimal for detection, since the rate of stopped gluino decays during any gap is essentially constant (once the number of stopped gluinos in the detector reaches saturation). The curves for 1 μs and 1 h are the first departures from this representative curve. It should also be noted that sensitivity to very short lifetimes will be affected by the length and number of gaps in the LHC filling scheme.

Interestingly, the discovery potential is much worse than one might naively think at an instantaneous luminosity of 10^{31} cm^{-2}. This is because, unlike collision produced backgrounds in an orthodox particle physics search, our backgrounds (instrumental noise and cosmics) have a rate which is independent of luminosity. Thus, for a counting experiment integrated over running time t, we have:

$$\frac{S}{\sqrt{B}} \propto \frac{\mathcal{L} \times t}{\sqrt{t}} \propto \mathcal{L}\sqrt{t}$$

So the expected significance, after running for a given period scales with the luminosity, but the running time required to achieve a given significance goes with the square of the luminosity. This differs from a normal particle physics analysis for which the expected significance goes like $\sqrt{\mathcal{L} \times t}$, and the running time required to achieve a given significance scales linearly with luminosity. We show the time to reach a 95% C.L. exclusion of the signal+background hypothesis during both beam gaps and interfill periods in a combined counting experiment for an instantaneous luminosity of 10^{31} cm^{-2} in Figure 8.

The model reach of the experiment can be expressed in terms of the sensitivity to gluino and neutralino masses, $m_{\tilde{g}}$ and $M_{\tilde{\chi}}$. Figure 9 show the significance that can be achieved after 30 days running as a function of the gluino mass, $m_{\tilde{g}}$. Figure 10 show the significance that can be achieved after 7 days running as a function of the neutralino mass, $M_{\tilde{\chi}}$. The dominant factors limiting the observable range of $m_{\tilde{g}}$ and $M_{\tilde{\chi}}$ are the signal cross-section and visible energy, respectively.

8 Sources of Systematic Uncertainty

The generic search for stopped particles described in this note is, by design, minimally exposed to systematic uncertainties. Since it will be conducted during beam-off periods, the cosmic ray + instrumental rate measured in CRAFT data as detailed in Section 5 exactly describes the background contribution to the search. The only uncertainties are statistical, and these are small.

The results of the sensitivity of the search to a particular model, e.g. split supersymmetry, as described in Section 7, however, do have some significant systematic uncertainties associ-

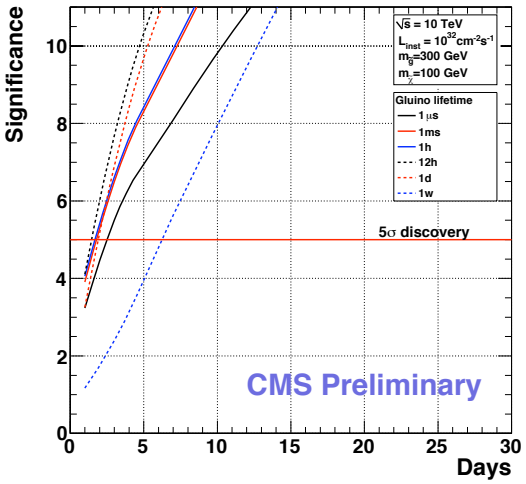

Figure 7: Discoverability during both beam gaps and interfill periods in a combined counting experiment. Assumes instantaneous luminosity of 10^{32} cm^{-2}. Note that the 1 ms curve is representative of a range from 10 μs to 100 s, for reasons explained in the text.

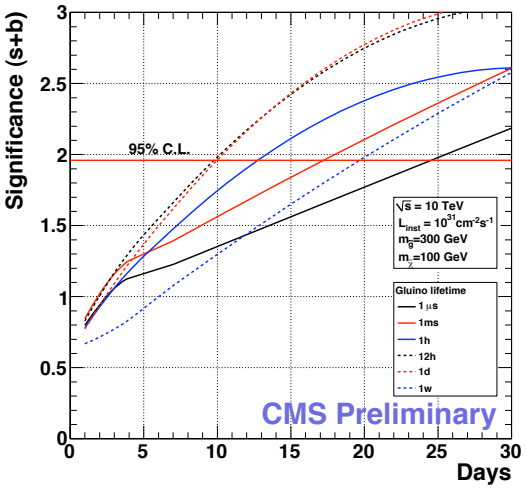

Figure 8: Time to reach 95% C.L. exclusion (of signal + background hypothesis) for both beam gaps and interfill periods in a combined counting experiment. Assumes instantaneous luminosity of 10^{31} cm^{-2}. Note that the 1 ms curve is representative of a range from 10 μs to 100 s, for reasons explained in the text.

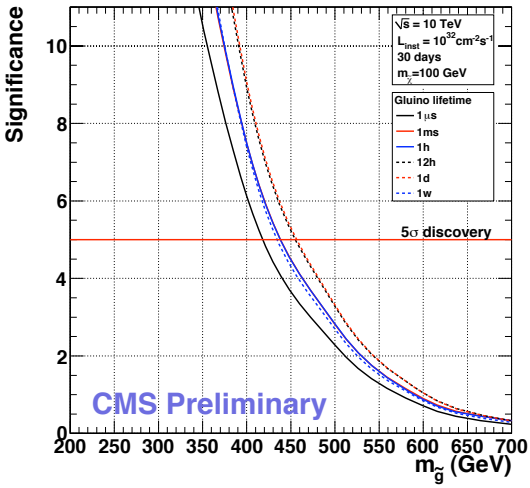

Figure 9: Significance achievable after 30 days running, as a function of gluino mass from a counting experiment using both beamgap and interfill periods. Note that the 1 ms curve is representative of a range from 10 μs to 100 s, for reasons explained in the text.

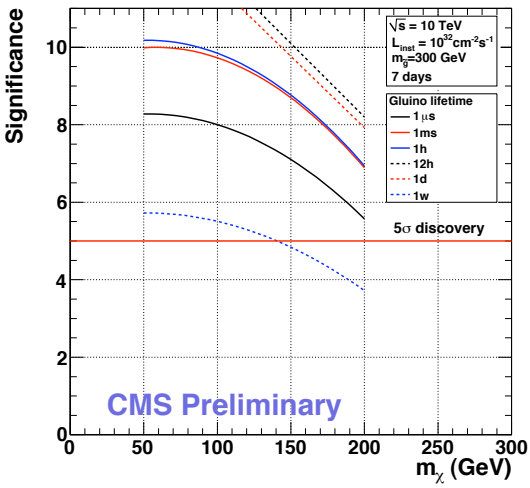

Figure 10: Significance achievable as a function of neutralino mass, from a counting experiment using both beamgap and interfill periods, after 7 days running. A gluino mass of 300 GeV is assumed. Note that the 1 ms curve is representative of a range from 10 μs to 100 s, for reasons explained in the text.

ated with them. In particular, the expected signal yield is sensitive to theoretical uncertainties involved in the NLO calculation of $\sigma(pp \to \tilde{g}\tilde{g})$ [6]. The theoretical uncertainties in this calculation arise from the choice of renormalisation/factorisation scales (10-15%) and proton parton distribution functions ($\sim$ 13%). The signal yield is also sensitive to the simulated stopping efficiency. The GEANT simulation used to derive the stopping efficiency implements models for both electromagnetic and nuclear interaction energy loss mechanisms. Whereas the EM model has been extremely well tested in previous experiments, and is based on known physics, the R-hadron "cloud model" used for NI has never been tested and is based on speculative physics extrapolated from low-energy QCD. We therefore assign a large systematic uncertainty to the stopping efficiency, taking the value obtained using EM interactions only as a lower limit, and that obtained with the full EM+NI interaction simulation as an upper limit (see Figure 2). This is the dominant uncertainty.

The results of the sensitivity of the stopped particle search presented in Section 7 are also sensitive to several operational assumptions made in the derivation of these results. A 12 hour interfill period, during which the stopped particle trigger had 100% live-time was assumed. If this is not the case for any of a number of reasons (e.g. quicker re-injection by LHC, conflict of trigger live-time with calibrations, etc.) the resultant sensitivity will degrade. This effect is most significant (for moderate lifetime particles) if the period immediately after the fill is not available for triggering. This effect is not, however, a true systematic error in the search, so no effort is made to quantify this effect, and no uncertainty is assigned. Finally, an average instantaneous luminosity was assumed, i.e. no attempt was made to model the exponential decay of the instantaneous luminosity. The effect of this omission is estimated to be $\pm$20%.

Table 2 summarises the sources of systematic uncertainty in the expected sensitivity of the stopped particle search. We illustrate the effect of these systematic uncertainties on the discovery potential for the combined beam gap and interfill period gap counting experiment in Figure 11.

Table 2: Potential Sources of Systematic Uncertainties in the Expected Sensitivity of the Stopped Particle Search

Source of Systematic Error	Estimated Fractional Uncertainty
PDF uncertainty on $\sigma(pp \to \tilde{g}\tilde{g})$ at NLO	$\pm$13%
Scale uncertainty on $\sigma(pp \to \tilde{g}\tilde{g})$ at NLO	$\pm 5 - 10\%$
Theoretical Uncertainty on Stopping Efficiency (Cloud Model)	-60%
Uncertainty on Background Rate	$< 1\%$
Uncertainty on Duration of Interfill Period	*
Uncertainty on Trigger live-time during Interfill Period	*
Uncertainty on Instantaneous Luminosity	$\pm$20%

9 Summary and Outlook

In this note we have presented plans for a search for long-lived particles which have become stopped by the CMS detector. We have described a novel calorimeter trigger that will allow us to record the subsequent decay of these stopped particles during time intervals where there are no pp collisions in CMS. We search for decays during empty buckets in the LHC beam structure as well as the inter-fill period between the beam being dumped and re-injection and thus achieve sensitivity to 12 orders of magnitude in stopped particle lifetime. We have developed

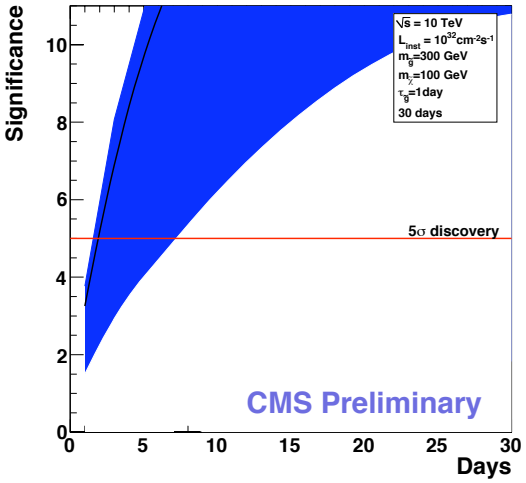

Figure 11: Discoverability of a 300 GeV gluino, with a lifetime of 1 day, from a counting experiment using both beamgap and interfill periods. Assumes instantaneous luminosity of 10^{32} cm^{-2}. Systematic uncertainty in the discoverability is indicated by the blue band.

a custom Monte Carlo simulation which allows us to estimate our signal efficiency. We have measured our backgrounds (instrumental noise in the CMS HCAL and cosmic rays) using pre-collision cosmic-ray data. We have combined this with our signal estimates to quantify our discovery reach. For models with relatively large cross-sections ($\sim$ 1 nb) we find we have the potential to make a 5 sigma discover in a matter of days with an instantaneous luminosity of 10^{32} cm^{-2}. This sensitivity improves greatly on that achieved in previous experiments [7], in part because of the novel triggering strategy that has been implemented.

References

[1] N. Arkani-Hamed and S. Dimopoulos, "Supersymmetric unification without low energy supersymmetry and signatures for fine-tuning at the LHC," *JHEP* **06** (2005) 073, arXiv:hep-th/0405159.

[2] **CMS** Collaboration, R. Adolphi et al., "The CMS experiment at the CERN LHC," *JINST* **0803** (2008) S08004. doi:10.1088/1748-0221/3/08/S08004.

[3] A. Arvanitaki, C. Davis, P. W. Graham, A. Pierce, and J. G. Wacker, "Limits on split supersymmetry from gluino cosmology," *Phys. Rev.* **D72** (2005) 075011, arXiv:hep-ph/0504210. doi:10.1103/PhysRevD.72.075011.

[4] A. Arvanitaki, S. Dimopoulos, A. Pierce, S. Rajendran, and J. G. Wacker, "Stopping gluinos," *Phys. Rev.* **D76** (2007) 055007, arXiv:hep-ph/0506242. doi:10.1103/PhysRevD.76.055007.

[5] R. Mackeprang and A. Rizzi, "Interactions of coloured heavy stable particles in matter," *Eur. Phys. J.* **C50** (2007) 353–362, arXiv:hep-ph/0612161. doi:10.1140/epjc/s10052-007-0252-4.

[6] W. Beenakker, R. Hopker, M. Spira, and P. M. Zerwas, "Squark and gluino production at hadron colliders," *Nucl. Phys.* **B492** (1997) 51–103, arXiv:hep-ph/9610490. doi:10.1016/S0550-3213(97)00084-9.

[7] **D0** Collaboration, V. M. Abazov et al., "Search for stopped gluinos from $p\bar{p}$ collisions at $\sqrt{s}$ = 1.96-TeV," *Phys. Rev. Lett.* **99** (2007) 131801, arXiv:0705.0306. doi:10.1103/PhysRevLett.99.131801.

A High Statistics Maps of Stopping Locations

In Figure 12, we present a higher statistics version of Figure 1 shown in Section 2. We also present the xy view of this stopping map in Figure 13.

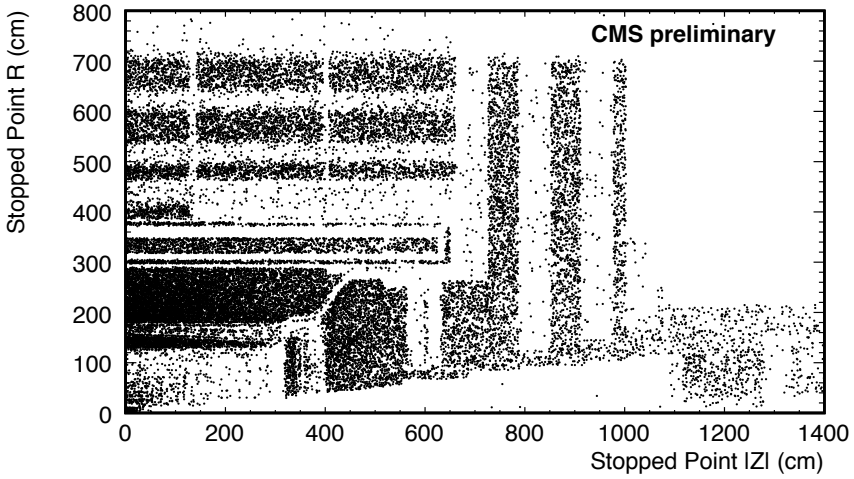

Figure 12: High statistics map of R-hadron stopping points for $m_{\tilde{g}} = 300$ GeV, and $\sqrt{s} = 10$ TeV in the $R - |z|$ plane.

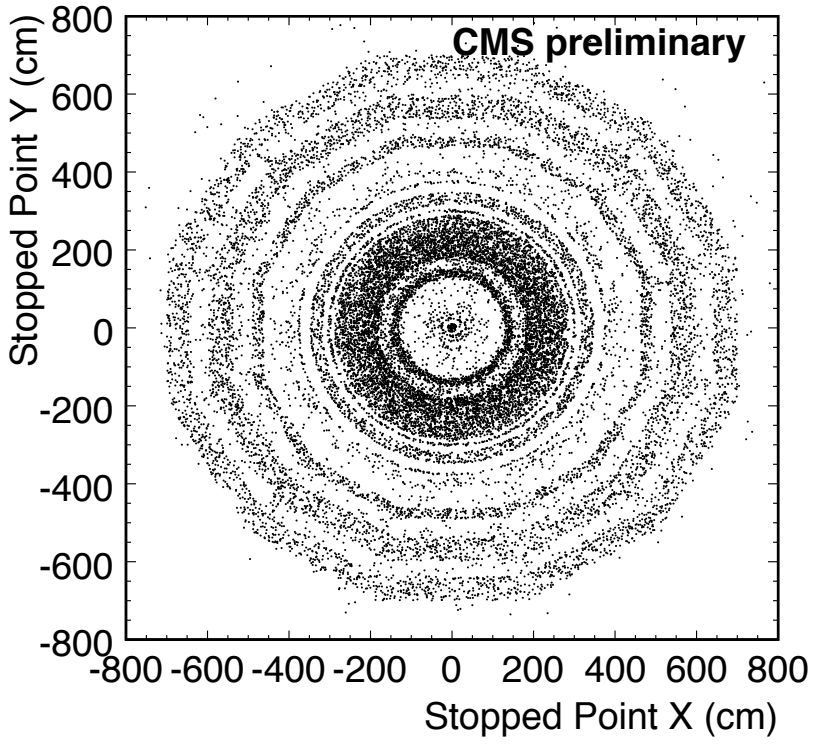

Figure 13: High statistics map of R-hadron stopping points for $m_{\tilde{g}} = 300$ GeV, and $\sqrt{s} = 10$ TeV in the $x - y$ plane.